Progress In Electromagnetics Research, Vol. 135, 465–480, 2013

USING WAVE-COEFFICIENTS AS FEATURE VECTORS TO IDENTIFY AEROSPACE TARGETS

Xiaomin Jiang[1], Shouqing Jia[1], Mingyao Xia[2, *], and Chihou Chan[3]

[1]School of Electronics Engineering and Computer Science, Peking University, Beijing 100871, China

[2]School of Electronic Engineering, University of Electronic Science and Technology of China, Chengdu 611731, China

[3]Department of Electronic Engineering, City University of Hong Kong, Hong Kong, China

Abstract—An original target identification method using Wave-Coefficients (WCs) as feature vector is proposed. The scattering fields of arbitrary shaped targets are expressed as a sum of spherical waves and the distinctive coefficients are exploited as the target feature. Decision rule based on correlation coefficient is established, and some analyses on the properties of the WCs are conducted. Numerical simulations of four targets are carried out and the recognition performances without and with noise are provided and discussed.

1. INTRODUCTION

Target identification has been a hot topic even since the invention of radar. It includes two essential steps: (1) selection and acquisition of feature vectors for the known targets to form a training database, and (2) extraction of feature vector from received responses and comparison with those of stored targets to make a decision by some rules.

The radar target identification can be realized using various target features, such as high resolution range profiles (HRRP) [1–5], synthetic aperture radar (SAR) [6–9] and inverse synthetic aperture radar (ISAR) [10, 11] images, natural frequencies [12–16] and the RCS (radar cross section) data [17]. The HRRPs and RCSs of a target are easy to get, but are highly sensitive to the orientation of the targets. The

Received 18 November 2012, Accepted 25 December 2012, Scheduled 26 December 2012

* Corresponding author: Mingyao Xia (myxia@uestc.edu.cn).

SAR and ISAR images are usually used for ship target identification. However, the obtaining of SAR and ISAR images is usually time-consuming and sometimes difficult. Identification methods based on the natural frequencies were considered to be promising, either by directly matching the natural frequencies or via the E-pulse techniques, because the natural frequencies are independent of the target-aspect. However, the energy contained in the late-time part is too weak and high Signal-to-Noise-Ratio (SNR) is hard to achieve.

In this paper, we develop a new target identification method based on wave-coefficients. The concept of wave-coefficients of two-dimensional (2D) objects was advanced in [18] and extended to three-dimensional (3D) objects in [19]. The proposed method can be applied to any a frequency range, with increased insensitivity to aspect angle at lower frequencies. However, if the frequencies are chosen too low, the targets are equivalent to point target, the proposed wave-coefficients do not embrace enough target discriminant information for recognition. The frequency range in resonance region is suggested in this paper. Simulation results show that the wave-coefficients can tolerate big aspect variation, yielding a significant advantage in saving memory space for establishing the template database. A simple decision rule based on correlation coefficient is established. Numerical experiments of four targets are conducted and identification performances with and without noise using the proposed scheme are presented.

In the following, Section 2 formulates the methodology. Section 3 presents the classifier and the recognition scheme. Some analyses on the properties of the WCs and recognition performances with and without noise based on WCs are given in 4. Finally, Section 5 is reserved for some concluding remarks.

2. BASIC PRINCIPLES

Consider that a plane wave is impressing on a conducting target with arbitrary shape. If the target were a sphere, the incidence were along the z-axis, and the electric field were polarized in x-direction, the scattered field of θ-component can be written as [20]

$$E_\theta^s = -\frac{E_0 \cos\phi}{kr} \sum_{n=1}^{\infty} j^n \frac{(2n+1)}{n(n+1)} \left\{ P_n a_n \hat{H}_n^{(2)}(kr) P_n^{(1)}(\cos\theta) - jQ_n b_n \hat{H}_n^{(2)'}(kr) \left[\cos\theta P_n^{(1)}(\cos\theta) - \gamma_n P_n^2(\cos\theta) \right] \right\} \quad (1)$$

where $\gamma_n = 0$ if $n = 1$ and 1 otherwise, and the coefficients P_n's and Q_n's are identically to be 1 for a sphere target. $k = \omega/c$ is the wave number, r the distance between radar and the target, and a_e

an effective radius defined by $a_e = d/2$ with d the minimum diameter of the sphere that encloses the target. $\hat{J}_n(\chi)$ and $\hat{H}_n^{(2)}(\chi)$ are the Ricatti-Beseel and Rcatti-Hankel functions defined as $\hat{J}_n^{(2)}(\chi) = \chi j_n(\chi)$ and $\hat{H}_n^{(2)}(\chi) = \chi h_n^2(\chi)$ with $j_n(\chi)$ and $h_n^2(\chi)$ the spherical Bessel and Hankel functions, respectively. $P_n^m(\cos\theta)$ is the associated Legendre Polynomial, and $P_n^{(1)}(\cos\theta) = \partial P_n^1(\cos\theta)/\partial(\cos\theta)$. The a_n and b_n in (1) are

$$a_n(k) = \hat{J}_n(ka_e)/\hat{H}_n^{(2)}(ka_e), \quad b_n(k) = \hat{J}_n'(ka_e)/\hat{H}_n^{(2)'}(ka_e) \tag{2}$$

In practice, the target is not a sphere, and the incidence is also arbitrarily relative to the orientation of the target. However, we may still write the scattered fields in the same form as (1) by modifying the coefficients P_n's and Q_n's, which are called the Wave-Coefficients (WCs) in this work. They are assumed to be dependent on the incident direction, but not sensitive to the angular frequency ω. Radar target recognition is usually a far-field inverse scattering problem, thus using the asymptotic formula

$$\hat{H}_n^{(2)}(\chi) = \chi h_n^{(2)}(\chi) = \sqrt{\frac{\pi\chi}{2}} H_{n+\frac{1}{2}}^{(2)}(\chi) = e^{-j(\chi - n\pi/2 - \pi/2)} \tag{3}$$

and substituting it into (1), we get

$$\begin{aligned} \tilde{E}_\theta^s \;=\; & \frac{jE_0\cos\phi}{k}\sum_{n=1}^{\infty}\frac{(2n+1)}{n(n+1)}\Big\{P_n a_n P_n^{(1)}(\cos\theta) \\ & + Q_n b_n\Big[\cos\theta P_n^{(1)}(\cos\theta) - \gamma_n P_n^2(\cos\theta)\Big]\Big\} \end{aligned} \tag{4}$$

where $\tilde{E}_\theta^s = E_\theta^s \cdot r/e^{-jkr}$. The WCs may be extracted by many means, and a way termed "Galerkin match" is suggested in this study. Actually, $\tilde{E}_\theta^s$ may be seen as an expansion by the "basis" functions $a_n(k)$ and $b_n(k)$, thus, we match (4) by using the same "basis" function as the "weighting" functions. Multiply both sizes of (4) by $a_m^*(k)$ and $b_m^*(k)$, where "$*$" denotes the complex conjugate, and integrate over the frequency band. We have

$$\sum_{n=1}^{2N} C_{mn}B_n = g_m, \quad m = 1, 2, \ldots, M, \;\; M \geq N \tag{5}$$

where N is the truncation terms, and B, g_m and C_{mn} are given as follows:

$$B_n = \begin{bmatrix} P_n \\ Q_n \end{bmatrix}, \quad C_{mn} = \begin{bmatrix} C_{mn}^1 \\ C_{mn}^2 \end{bmatrix}, \quad \text{and} \quad g_m = \begin{bmatrix} g_m^1 \\ g_m^2 \end{bmatrix} \tag{6}$$

with

$$C^1_{mn} = \begin{cases} jE_0 \cos\phi P_n^{(1)}(\cos\theta) \frac{(2n+1)}{n(n+1)} \int_{k_{\min}}^{k_{\max}} a_m^*(k) * a_n(k)dk, \\ \qquad\qquad 1 \le n \le N \\ jE_0 \cos\phi \cos\theta P_1^{(1)}(\cos\theta) \frac{(2n+1)}{n(n+1)} \int_{k_{\min}}^{k_{\max}} a_m^*(k) * b_1(k)dk, \\ \qquad\qquad n = N+1 \\ jE_0 \cos\phi \frac{(2n+1)}{n(n+1)} \left[\cos\theta P_{n-N}^{(1)}(\cos\theta) - P_{n-N}^2(\cos\theta)\right] \\ \times \int_{k_{\min}}^{k_{\max}} a_m^*(k) * b_{n-N}(k)dk, \qquad N+2 \le n \le 2N \end{cases} \tag{7}$$

$$g^1_m = \int_{k_{\min}}^{k_{\max}} a_m^*(k) \cdot \tilde{E}_\theta^s(k)kdk \tag{8}$$

The C^2_{mn} and g^2_m are the same as C^1_{mn} and g^1_m just by replacing $a^*_m(k)$ with $b^*_m(k)$ in the formulae.

The left hand of (4) is obtained by numerical simulation using the method of moments (MoM). The Wave-Coefficients (WCs) are obtained through solving (5) by the method of least square (LS). The backscattering ($\phi - \phi_i = \pm\pi$, $\theta + \theta_i = \pi$) circumstance is considered in this study. It should be mentioned that if the actually received fields in time domain is $E^R_\theta(t)$, then $E^s_\theta(\omega) = E^R_\theta(\omega)/A(\omega)$ is used, where $E^R_\theta(\omega)$ is the frequency spectrum of $E^R_\theta(t)$ and $A(\omega)$ is the frequency spectrum of the radar waveform.

3. CLASSIFIER AND RECOGNITION SCHEME

The right hand of Equation (5) varies with the incident angle, while C_{mn} is independent of the incident angle; consequently, the WCs change with the incident angle. The Correlation Coefficient is used to evaluate the similarity of two feature vectors (namely two set of WCs in this work). Let $\mathbf{B}(i,j) = \{B_n(i,j) : n = 0, 1, \ldots, N\}$be the j-th feature vector stored in the database for the target i, and let $\mathbf{X} = \{X_n : n = 0, 1, \ldots, N\}$ be an incoming feature vector belonging to an unknown target to be compared. The Correlation Coefficient is defined as

$$C(i,j;\mathbf{X}) = \frac{\left|\sum_{n=0}^{N} B_n(i,j) \cdot X_n^*\right|}{\sqrt{\sum_{n=0}^{N} |B_n(i,j)|^2 \cdot \sum_{n=0}^{N} |X_n|^2}} \tag{9}$$

where the asterisk denotes the complex conjugate. It is clear that $0 \le C \le 1$ and $C = 1$ if and only if the two feature vectors are

in proportion. The Correlation Coefficient is an intuitive measure of similarity between the two feature vectors. As a result, for a pre-estimated incident direction denoted by j_0, the Correlation Coefficient value for the target i is $C(i, j_0; \mathbf{X})$, and the unknown target will be judged to be the target i_0 if the maximum Correlation Coefficient value is produced for $i = i_0$.

Using the above decision rule, the proposed recognition procedure goes as follows:

Step 1: Build the database containing the WCs of K preselected targets at aspects of interest. Denote it by $\mathbf{B}_i(\theta, \phi)$ for each target i at the azimuth (θ, ϕ). The sampling interval $\delta\theta$ and $\delta\phi$ is determined by the WCs' sensitivity to incident angle θ and ϕ which is studied in the next section.

Step 2: Obtain the input WC $\mathbf{X}(\theta_0, \phi_0)$ of an unknown target and estimate its aspect (θ_0, ϕ_0) with respect to the radar. Denote them by $(\tilde{\theta}_0, \tilde{\phi}_0)$.

Step 3: Suppose the estimated errors are within $\pm\Delta\theta$ and $\pm\Delta\phi$, respectively. Find all $\left\{\mathbf{B}_i(\theta, \phi)/\tilde{\theta}_0 - \Delta\theta \le \theta \le \tilde{\theta}_0 + \Delta\theta, \tilde{\phi}_0 - \Delta\phi \le \phi \le \tilde{\phi}_0 + \Delta\phi\right\}$ from the database, and compute the Correlation Coefficient $\{C(\mathbf{X}, B_i)/1 \le i \le K\}$.

Step 4: Identify the unknown target to be the one that has the maximum Correlation Coefficient.

4. NUMERICAL EXPERIMENTS

Consider the coordinate system shown in Figure 1. The spherical coordinate system is defined as (r, θ, ϕ) where r is the distance from the observation point to origin, θ is the elevation angle and ϕ is the azimuthal angle. Assume that there are four types of known aircrafts including target No. 1, target No. 2, target No. 3 and target No. 4. The geometrical models for these four types of known planes are shown in Figure 2. The head of the plane is in the $-x$-direction, and the left-wing is in the y-direction. The centers of the planes coincide with the origin. They have the same length of 2.0 meters; their widths are 1.04 meters, 1.29 meters, 1.29 meters and 1.8834 meters, respectively; and their heights are 0.4 meters, 0.225 meters, 0.374 meters and 0.1 meters, respectively. The frequency band is chosen to be $300 \sim 600$ MHz in this paper.

In the following, the distinction of the wave-coefficient is discussed in Section 4.1. Then the WC's sensitivity to the aspect angle is detailedly investigated in Section 4.2. The identification performances

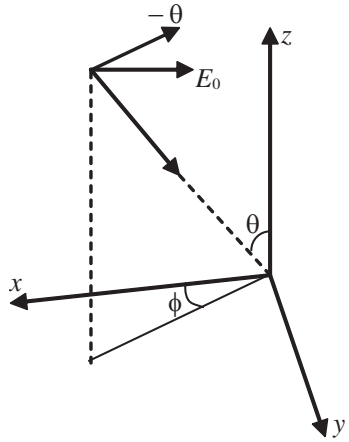

Figure 1. Coordinate system.

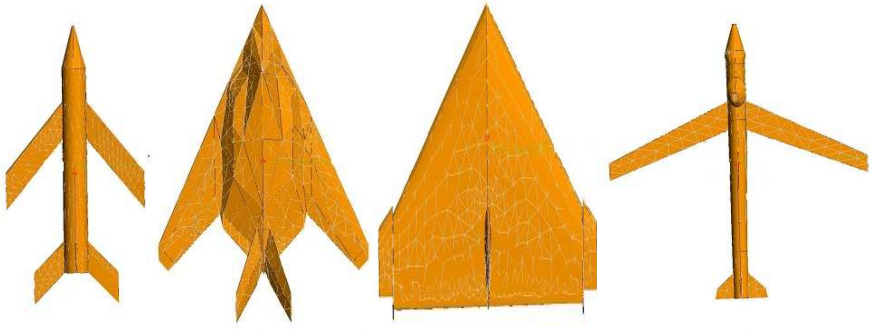

Figure 2. The geometrical models for the four types of known planes: (a) Target No. 1, (b) target No. 2, (c) target No. 3, and (d) target No. 4.

based on WCs without and with noise will be presented in Sections 4.3 and 4.4, respectively.

4.1. Distinction of the Wave-coefficient

The truncation term is taken to be $N = 20(P_n : 1 \leq n \leq 20,\ Q_n : 1 \leq n \leq 20)$, so that only 40 coefficients are extracted. The typical WCs of the target No. 1 and target No. 3 are shown in Figure 3.

From Figure 3 we can see that the WCs of different targets have significant differences from each other, which indicates that the WCs have obvious target distinction.

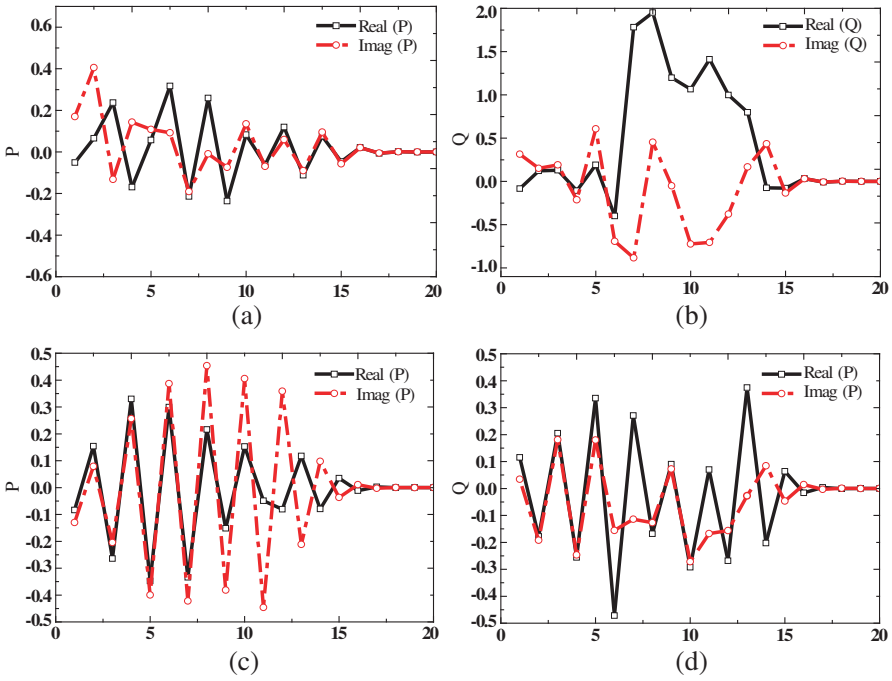

Figure 3. The WCs for incident angle $\theta_i = 180°$, $\phi_i = 0°$: (a) P_n of target No. 1, (b) Q_n of target No. 1, (c) P_n of target No. 3, and (d) Q_n of target No. 3.

4.2. The WCs' Sensitivity to Aspect Angle

The Correlation Coefficient is referred to as complex or absolute depending on whether the complex wave-coefficients or the absolute values of the wave-coefficients are used in the feature vector presentation. Both complex and absolute Correlation Coefficients of adjacent aspect are calculated to examine the tolerance of angular estimation errors. To study the WCs' sensitivity to the target-aspect, an angle matching width (AMW) is introduced. δ is a prescribed Correlation Coefficient threshold, matching width is defined as AMW $= \alpha_2 - \alpha_1$, where α_1 and α_2 are respectively the minimum and maximum values that satisfy

$$C\left(i_0, \alpha_l; \alpha_0\right) \geq \delta, \quad l = 1, 2 \tag{10}$$

in which α_0 is called the middle angle. Next, AMW for each target is examined in two middle elevation angles, they are $\theta_0 = 104°$ and $\theta_0 = 164°$, respectively. The azimuth search window is $\Delta\theta = \pm 10°$.

The results are plotted in Figure 4.

Figure 4 shows that the AMW varies from target to target. For a given target, the AMW changes along with the middle angle. Suppose that a matching tolerability of 10% is acceptable ($C > 0.90$). In Figure 4(a), the widest AMW for the four targets is wider than 20° and at least 16°; in Figure 4(b), the widest AMW for the four targets is wider than 16° and at least 6°; in Figure 4(c), the widest AMW for the four targets is wider than 20° and at least 18°; in Figure 4(d), the widest AMW for the four targets is wider than 20° and at least 16°. It can be seen that complex Correlation Coefficients are more sensitive to aspect. Therefore, a finer angular sampling interval would be required, leading to a bigger target database. On the other hand, the absolute identification has better tolerance of angular estimation error. When constructing the feature vector template database, if we investigate the matching width in all the aspect of interest (because

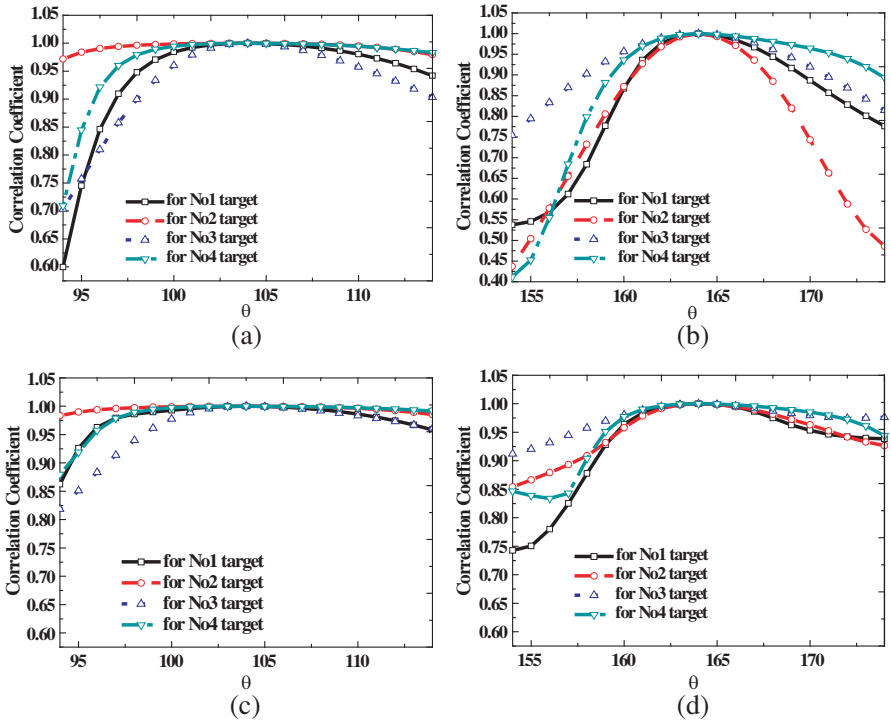

Figure 4. Complex (upper) and absolute (under) AMW for the targets: (a) Middle angle $\theta_0 = 104°$, (b) middle angle $\theta_0 = 164°$, (c) middle angle $\theta_0 = 104°$, (d) middle angle $\theta_0 = 164°$.

of symmetry, the aspect of interest is 0°–180°), the sampling interval $\delta\theta$ should vary with the aspect angle. Thus the number of template wave-coefficients stored in the data base for the targets can be greatly reduced.

4.3. Identification Performance Without Noise

For each object two independent experiments are carried out at two elevation angles: $\theta = 0°$ and 6°. For each elevation angle the object is rotated from $\phi = 0°$ to 180° with an increment of 10°. For convenience of description, we list the notations that will be used in the following. Table 1 lists the data set used. Each data set consists of wave-coefficients of four targets. A data set tag is appended to each name. For example, No. 2-2 denotes data of the second target in the data set DATA2.

In this subsection, we consider the situation in which the elevation angle of the input target is different from that of the database. The database is DATA-1, and the input vectors are from DATA-2. It is noted that there is a 6° difference in elevation between the target arrangements used in DATA-2 and DATA-1. The aspect angles for testing are uniformly sampled and they are $\phi = 5°, 15°, \ldots, 175°$. The complex and absolute Correlation Coefficients between the test target and the four known targets at all the 18 testing aspect angles are shown in Figure 5, the test target is supposed to be target No. 1. In Figure 5(a), the complex Correlation Coefficient is utilized. The average Correlation Coefficient of the 18 testing aspect angles is 0.9659 to target No. 1, 0.4706 to target No. 2, 0.4354 to target No. 3 and 0.4320 to target No. 4. In Figure 5(b), the absolute Correlation Coefficient is used. The average Correlation Coefficient of the 18 testing aspect angles is 0.9833 to target No. 1, 0.7503 to target No. 2, 0.6770 to target No. 3 and 0.8860 to target No. 4. Both figures show that the known target of No. 1 has the biggest Correlation Coefficient, i.e., resembles the test target most. The identification results are right at all the 18 testing aspect angles and then the successful identification rate is $18/18 = 100\%$. The discrimination capability can be defined as the discrepancy in the best and the second-best average Correlation

Table 1. Notation of the data set.

Data set	Elevation angle	Sampling increment in azimuth
DATA-1	0°	10°
DATA-2	6°	10°

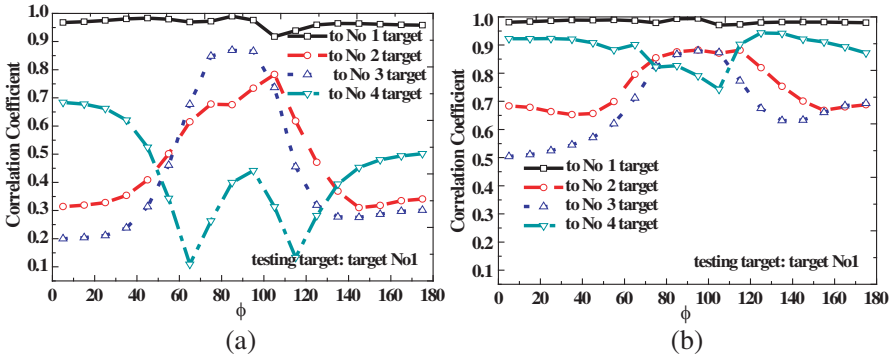

Figure 5. The Correlation Coefficients between the test target (i.e., target No. 1 in the first instance) and the four known targets at all the 18 testing aspect angle of ϕ: (a) Complex situation, (b) absolute situation.

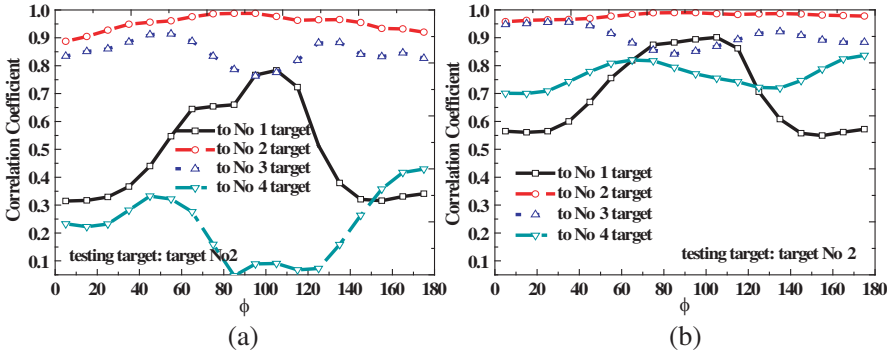

Figure 6. The Correlation Coefficients between the test target (i.e., target No. 2 in the second instance) and the four known targets at all the 18 testing aspect angle of ϕ: (a) Complex situation, (b) absolute situation.

Coefficient. Under this definition, the discrimination capability is 0.4953 for Figure 5(a), and is 0.0973 for Figure 5(b). This means that the complex Correlation Coefficient has better discriminating ability than absolute Correlation Coefficient. It is also seen from Figure 5(a) that significant differences exist between the matched and mismatched targets. On the other hand, the absolute identification is usually based on small or even negligible differences; however, as discussed above, this method has wider AMW.

In Figure 6, the test target is supposed to be target No. 2. In

Figure 6(a), the complex Correlation Coefficient is utilized. The average Correlation Coefficient of the 18 testing aspect angles is 0.5345 to target No. 1, 0.9506 to target No. 2, 0.8714 to target No. 3 and 0.3690 to target No. 4. In Figure 6(b), the absolute Correlation Coefficient is used. The average Correlation Coefficient of the 18 testing aspect angles is 0.6947 to target No. 1, 0.9785 to target No. 2, 0.9039 to target No. 3 and 0.7652 to target No. 4. Both results show that the known target of No. 2 resembles the test target most. The recognition results are correct at all the 18 testing aspect angles and then the successful identification rate is $18/18 = 100\%$. The discrimination capability is 0.0792 for Figure 6(a), and is 0.0746 for Figure 6(b). This means that the complex Correlation Coefficient has better discriminating ability than absolute Correlation Coefficient. We find that the discrimination capability is small mostly due to the structural similarity between No. 2 target and No. 3 target.

In Figure 7, the test target is supposed to be target No. 3. In Figure 7(a), the complex Correlation Coefficient is utilized. The average Correlation Coefficient of the 18 testing aspect angles is 0.4310 to target No. 1, 0.8018 to target No. 2, 0.9413 to target No. 3 and 0.4160 to target No. 4. In Figure 7(b), the absolute Correlation Coefficient is applied. The average Correlation Coefficient of the 18 testing aspect angles is 0.7047 to target No. 1, 0.9544 to target No. 2, 0.9768 to target No. 3 and 0.7394 to target No. 4. Both figures show that the known target of No. 3 resembles the test target most. The identification results are correct at all the 18 testing aspect angles for Figure 7(a) and then the successful identification rate is $18/18 = 100\%$, however, the

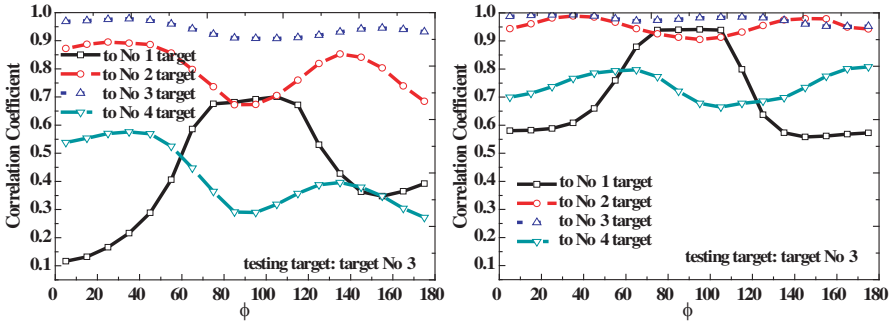

Figure 7. The Correlation Coefficients between the test target (i.e., target No. 3 in the third instance) and the four known targets at all the 18 testing aspect angle of ϕ: (a) Complex situation, (b) absolute situation.

recognition results are wrong at 2 testing aspect angles for Figure 7(b) and then the successful identification rate is 16/18 = 88.9%. The discrimination capability is 0.1395 for Figure 7(a), and is 0.0973 for Figure 7(b). This indicates that the complex Correlation Coefficient has better discriminating ability than absolute Correlation Coefficient. The discrimination capability is small mostly due to the structural similarity between No. 3 target and No. 2 target.

In Figure 8, the test target is supposed to be target No. 4. In Figure 8(a), the complex Correlation Coefficient is utilized. The average Correlation Coefficient of the 18 testing aspect angles is 0.5846 to target No. 1, 0.2159 to target No. 2, 0.3787 to target No. 3 and 0.8710 to target No. 4. In Figure 8(b), the absolute Correlation Coefficient is applied. The average Correlation Coefficient of the 18 testing aspect angles is 0.8415 to target No. 1, 0.8055 to target No. 2, 0.7390 to target No. 3 and 0.9460 to target No. 4. Both figures show that the known target of No. 4 resembles the test target most. The recognition results are right at all the 18 testing aspect angles and then the successful identification rate is 18/18 = 100%. The discrimination capability is 0.2864 for Figure 8(a), and is 0.1045 for Figure 8(b). This means that the complex Correlation Coefficient has better discriminating ability than absolute Correlation Coefficient. It is also seen from Figure 8(a) that significant differences exist between the matched and mismatched targets. On the other hand, the absolute identification is based on small differences.

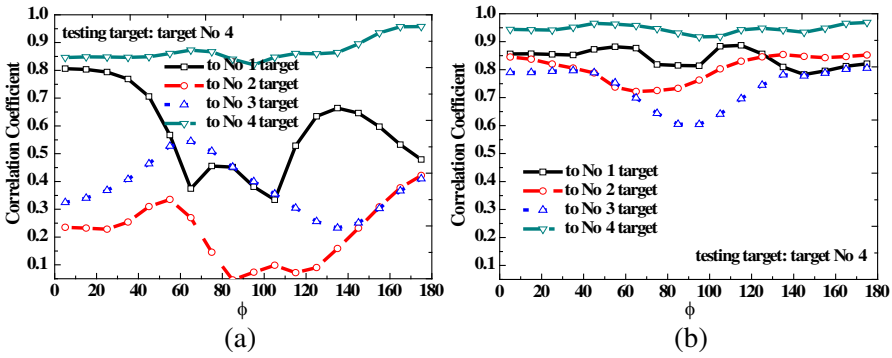

Figure 8. The Correlation Coefficients between the test target (i.e., target No. 4 in the fourth instance) and the four known targets at all the 18 testing aspect angle of ϕ: (a) Complex situation, (b) absolute situation.

4.4. Identification Performance in the Presence of Gaussian Noise

To investigate the performance of the proposed scheme in a noisy environment, an additive white Gaussian noise (AWGN) model is assumed, and the noise-corrupted received fields on the left-hand side of (4) is taken to be

$$E_z^s(k_m) = E_z^{so}(k_m) + \nu_m, \quad m = 1, 2, \ldots, n\_freq \tag{11}$$

where n_freq is the number of frequency points, $E_z^{so}(k_m)$ is the noiseless fields, i.e., the theoretical fields received by simulations, and $\nu_m = \nu_m^R + j\nu_m^I$ is a complex white Gaussian noise, i.e., both sequences $\{\nu_m^R : m = 1, 2, \ldots n\_freq\}$ and $\{\nu_m^I : m = 1, 2, \ldots, n\_freq\}$ have zero mean values and variances $\rho^2/2$ with ρ^2 being the noise power

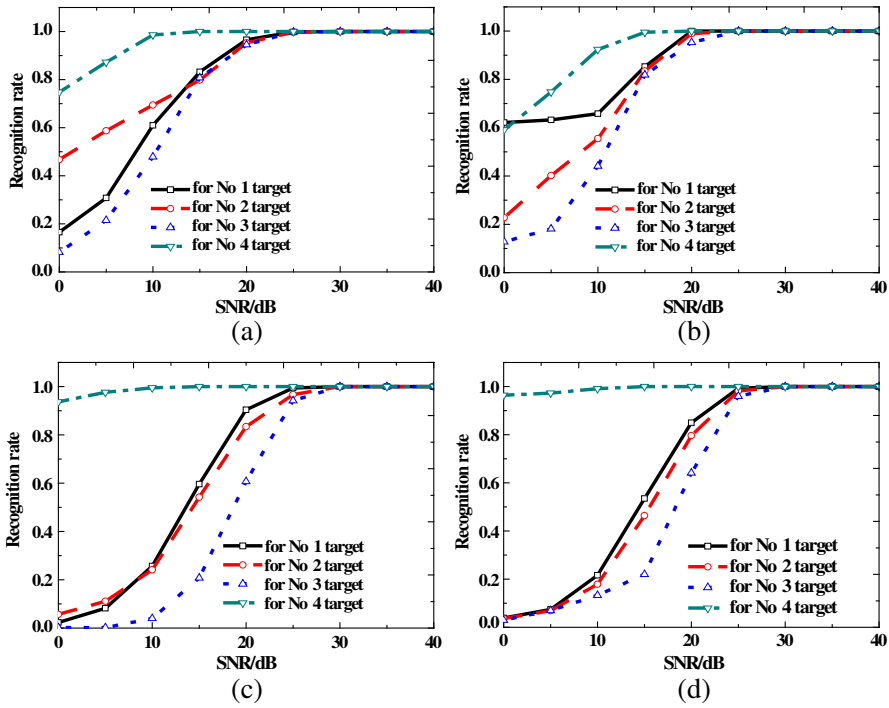

Figure 9. The successful identification rate with respect to SNR: (a) $\phi_i = 90°$, complex Correlation Coefficient, (b) $\phi_i = 75°$, complex Correlation Coefficient, (c) $\phi_i = 90°$, absolute Correlation Coefficient, (d) $\phi_i = 75°$, absolute Correlation Coefficient.

calculated by

$$\rho^2 = P_0 \times 10^{-(\mathrm{SNR}/10)} \tag{12}$$

in which P_0 is the power of the noiseless sequence $\{E_z^{so}(k_m) : m = 1, 2, \ldots, n\_freq\}$, and SNR (in dB) is the Signal-to-Noise-Ratio to be assigned. In the following computations, the SNR is varied from 0 to 40 dB with 5 dB steps.

The coefficients at two typical azimuths of $\phi_i = 90^\circ$ and $\phi_i = 75^\circ$ from DATA-1 are taken as examples to examine the performance of our wave-coefficients approach in the presence of additive, zero-mean, complex Gaussian noise. The noise-contaminated complex or absolute wave-coefficients are correlated with DATA-1. One thousand simulations are conducted. The successful identification rate at different noise levels are plotted in Figure 9. Comparing Figure 9(a) and Figure 9(c), Figure 9(b) and Figure 9(d), we find that the complex method is more tolerant of additive noise than the absolute method. This result is mainly due to better discriminating capability for complex Correlation Coefficient technique.

5. CONCLUDING REMARKS

The backscattering fields from 3D targets with arbitrarily shape can be expressed as a sum of spherical wave-modes. The expansion wave-coefficients have some distinctive properties and may be exploited as feature vectors for target identification. The Correlation Coefficient of two feature vectors is taken to be as the identification decision rule. The absolute Correlation Coefficient technique is tolerant of angular estimation error, but the discriminating capability is somewhat too small. The complex correlation coefficient method can provide more reliable identification. However, it requires comparatively small aspect increment. The encouraging result is that a fairly wide AMW exists even for complex Correlation Coefficient method, thus the number of template feature vectors stored for each target is acceptable. This technique is especially suitable for recognition of aerospace targets because their postures and velocities can be estimated to some extent. The time to search the corresponding template feature vectors stored in the target database and calculate the Correlation Coefficients can therefore be fast enough in real applications. The successful recognition rate in noise environment depends not only on the noise level, but also on the discriminating capability. Further investigation of the proposed approach, such as using other algorithms for extraction and the other decision rules for classification are in progress.

ACKNOWLEDGMENT

This work is supported by NSFC Projects 60825102 and 61271032.

REFERENCES

1. Li, H. J. and S. H. Yang, "Using range profiles as feature vectors to identify aerospace objects," *IEEE Transactions on Antennas and Propagation*, Vol. 41, No. 3, 261–268, 1993.
2. Du, L., H. W. Liu, Z. Bao, and M. D. Xing, "Radar HRRP target recognition based on higher order spectra," *IEEE Trans. on Signal Processing*, Vol. 53, No. 7, 2359–2368, 2005.
3. Liu, H. W. and Z. Bao, "Radar HRR profiles recognition based on SVM with power-transformed-correlation kernel," *Springer Lecture Notes in Computer Science*, 531–536, Springer-Verlag, Berlin, 2004.
4. Han, S. K. and H. T. Kim, "Efficient radar target recognition using a combination of range profile and time-frequency analysis," *Progress In Electromagnetic Research*, Vol. 108, 131–140, 2010.
5. Kim, K. T., D. K. Seo, and H. T. Kim, "Efficient radar target recognition using the MUSIC algorithm and invariant feature," *IEEE Transactions on Antennas and Propagation*, Vol. 50, No. 3, 325–337, 2002.
6. Zhao, Q. and J. C. Principle, "Support vector machines for SAR automatic target recognition," *IEEE Transactions on Aerospace and Electronic Systems*, Vol. 37, No. 2, 643–654, 2001.
7. Huan, R. H. and Y. Pan, "Target recognition for multi-aspect SAR images with fusion strategies," *Progress In Electromagnetic Research*, Vol. 134, 267–288, 2013.
8. Chang, Y. L., C. Y. Chiang, and K. S. Chen, "SAR image simulation with application to target recognition," *Progress In Electromagnetic Research*, Vol. 119, 35–57, 2011.
9. Zhai, Y., J. Li, J. Gan, and Z. Ying, "A multi-scale local phase quantization plus biomimetic pattern recognition method for SAR automatic target recognition," *Progress In Electromagnetic Research*, Vol. 135, 105–122, 2013.
10. Park, S.-H., J.-H. Lee, and K.-T. Kim, "Performance analysis of the scenario-based construction method for real target ISAR recognition," *Progress In Electromagnetic Research*, Vol. 128, 137–151, 2012.
11. Park, J. I. and K. T. Kim, "A comparative study on ISAR

imaging algorithm for radar target identification," *Progress In Electromagnetic Research*, Vol. 108, 155–175, 2010.

12. Baum, C. E., E. J. Rothwell, K. M. Chen, and D. P. Nyquist, "The singularity expansion method and its application to target identification," *IEEE Proceedings*, Vol. 79, No. 10, 1481–1491, 1991.
13. Wang, S. G., X. P. Guan, X. Y. Ma, D. W. Wang, and Y. Su, "Calculating the poles of complex radar target," *Journal of Electromagnetic Waves and Applications*, Vol. 20, No. 14, 2065–2076, 2006.
14. Lui, H. S. and N. Shuley, "Radar target identification using a 'Banded' E-pulse technique," *IEEE Transactions on Antennas and Propagation*, Vol. 54, No. 12, 3874–3881, 2006.
15. Lee, J. H., S. W. Cho, S. H. Park, and K. T. Kim, "Performance analysis of radar target recognition using natural frequency: frequency domain approach," *Progress In Electromagnetic Research,* Vol. 132, 315–345, 2012.
16. Morales, J. D., D. Blanco, D. P. Ruiz, and M. C. Carrion, "Radar-target identification via exponential extinction-pulse synthesis," *IEEE Transactions on Antennas and Propagation*, Vol. 55, No. 7, 2064–2072, 2007.
17. Huang, C. W. and K. C. Lee, "Application of ICA technique to PCA based radar target recognition," *Progress In Electromagnetic Research*, Vol. 105, 157–170, 2010.
18. Jiang, X. M., S. Q. Jia, and M. Y. Xia, "Reconstruction of scattering fields using wave-mode coefficients for 2D conducting targets," *Cross Strait Quad-Regional Radio Science and Wireless Technology Conference*, 64–67, Harbin, China, 2011.
19. Jiang, X. M. and M. Y. Xia, "A study of wave coefficients as target signature for identification," *IEEE International Symposium on Antennas and Propagation*, Chicago, USA, July 2012.
20. Stratton, J. A., *Electromagnetic Theory*, 1st edition, 664, Mc Graw-Hill, 1941.